Intelligent Modeling for Transfer Function Control of DBR Semiconductor Laser at Near-Working Point

XIUFEI LI[1], **ZHUO WANG**[2,3,4], **(Member, IEEE), LU YU**[1], **XIAOLIN NING**[2,3], **WEI QUAN**[2,3,4], **AND YUEYANG ZHAI**[2,3]

[1]School of Instrumentation Science and Opto-Electronics Engineering, Beihang University, Beijing 100191, China
[2]Beijing Academy of Quantum Information Sciences, Beijing 100193, China
[3]Research Institute for Frontier Science, Beihang University, Beijing 100191, China
[4]Key Laboratory of the Ministry of Industry, Beihang University, Beijing 100191, China

Corresponding authors: Zhuo Wang (zhuowang@buaa.edu.cn) and Yueyang Zhai (yueyangzhai@163.com)

ABSTRACT In this paper, a novel intelligent modeling method for transfer function control of DBR semiconductor lasers at near-working point is proposed, which is based on the quantum particle swarm optimization (QPSO) algorithm. This modeling method effectively solves the difficulty of application in the traditional laser theory and equivalent circuit models in practical engineering. First, we analyze the input and output characteristics of DBR semiconductor laser at near-working point, where the laser system can be equivalent to a transfer function model including two main modules: the laser power control module and the laser wavelength control module, and determine the structure of this equivalent model based on the analysis results. Then, we use the QPSO intelligent algorithm to identify the model parameters and finally obtain the equivalent transfer function model that can be easily applied to practical engineering. The standard deviations of the steady-state errors of these two modules are 3.4×10^{-3} and 1.2×10^{-5}, respectively. Experiments verify the effectiveness and convenience of the proposed (intelligent modeling) method, which can be used for on-line modeling of the DBR semiconductor laser at near-working point.

INDEX TERMS DBR semiconductor laser, transfer function control, laser power control module, laser wavelength control module, intelligent modeling.

I. INTRODUCTION

With the development of quantum information science and technology, a series of high precision quantum measurement instruments have been developed, such as atomic gyroscopes [1], [2], atomic magnetometers [3], [4], atomic clocks [5], [6] and atomic gravimeters [7], [8]. Quantum measurement instruments have the advantages of ultra-high measurement accuracy, which is an important research direction in the field of information and instrument science in the new century [9]–[11]. Most quantum measurement instruments use lasers to manipulate the quantum (atoms/photons/

electronics) for physical measurements, because of which high-performance laser is essential.

With the characteristic of miniaturization, semiconductor lasers can be widely used in future miniature quantum precision measurement sensors. Distributed Bragg reflector (DBR) semiconductor laser has narrow linewidth, allows for smooth, wide range wavelength tuning and less sensitive to ambient air temperature. Its performance is important to atomic inertial measurement. In order to make the DBR laser system work in an ideal state at the working point, transfer function control (TFC) method is needed. However, due to the complexity of the device structure of semiconductor laser and the complicated physical process of the interaction between photons and electrons, it is difficult to establish a proper and complete dual-input dual-output control system model that

The associate editor coordinating the review of this manuscript and approving it for publication was Guijun Li.

meets the requirement of quantum precision measurement. In this situation, a proper and accurate modeling method is necessary for the application of TFC method.

So far, the classical model of semiconductor laser is the equivalent circuit model [12]–[18], which is composed of two parts: the intrinsic part and the parasitic network part. In the equivalent circuit model, the intrinsic part reflects the optical-electrical characteristics of the semiconductor laser, while the parasitic network part has no business interfering with it [18] and thus will not be investigated in this paper. On one hand, the intrinsic part cannot be measured by using external measurements, but can only be modeled by solving the rate equation which is applicable to the semiconductor laser. However, the rate equation cannot fully reflect all the control characteristics of the semiconductor laser, because its solution conditions are based on some ideal approximations, where the influence of temperature on the laser output is not described [18]. Besides, the rate equation is obtained based on the single-mode operation whose working current is bigger than the threshold current, where the influence of the input on the output wavelength is ignored. On the other hand, there are mainly two categories of the equivalent circuit model: the large signal model [17] and the small signal model [19], which basically focus on reflecting the impedance characteristics and modulation characteristics of the semiconductor laser, respectively. However, neither the large signal model nor the small signal model reflects the temperature influence on the laser output. In addition, the small signal model even ignores the impedance of the intrinsic part, such that the optical characteristics (including the wavelength and power characteristics) of laser output are also ignored [19], [20].

In order to overcome the incompleteness of the traditional equivalent circuit model that ignores the temperature influence and the optical characteristics of the semiconductor laser, this paper proposes an intelligent modeling method for TFC of the DBR semiconductor laser. In view of the complexity of the interaction between photons and electrons, as well as the nonlinear time-varying relationship between the laser input and the laser output, we first linearize the system model at near-working point, so that a general model framework for TFC is constructed through the classical modeling method [21]–[24]. This general framework is composed of two main modules: the laser power control module and the laser wavelength control module, whose model parameters are unidentified. Then, the model parameters are identified by using the quantum particle swarm optimization (QPSO) method, which is a new particle swarm optimization method proposed by Sun Jun et al. from the perspective of quantum mechanics [25], [26]. This algorithm has been widely applied in the model parameter identification, whose main advantage is the excellent ability of global optimization that other intelligent algorithms cannot match [27]–[29]. Because of this, the QPSO algorithm is feasible to TFC of DBR semiconductor laser, since the parameter identification for the laser model is actually a global optimization problem [30], [31]. The proposed intelligent modeling method effectively
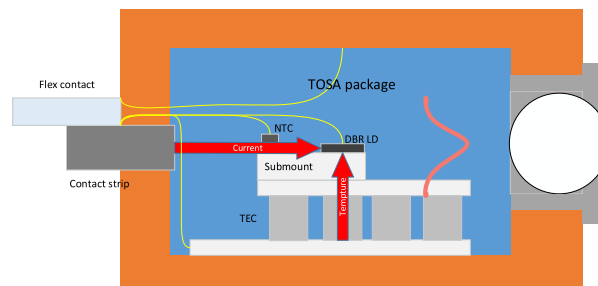

FIGURE 1. TOSA package DBR semiconductor laser. Here DBR LD: Distributed Bragg reflector semiconductor laser diode, NTC: Negative temperature coefficient thermistor, TEC: Thermo electric cooler.

overcomes the lack of the temperature item and the optical output items in the traditional equivalent circuit model, which is therefore more feasible and accurate for TFC of the DBR semiconductor laser.

II. METHODS
A. INTELLIGENT MODELING OF TRANSFER FUNCTION CONTROL MODEL FOR DBR NEAR THE WORKING POINT
DBR semiconductor laser has the characteristics of high photoelectric conversion efficiency, strong wavelength and power tuning ability and high reliability. Its performance is very important to atomic inertial measurement. The transmitter optical sub-assembly (TOSA) package DBR semiconductor laser has the characteristics of compact structure and high power (shown as FIGURE 1). In this paper, the TOSA package DBR semiconductor laser applied to the inertial measurement device is modeled. However, the small dimension of TOSA package increases the heat density generated in the DBR semiconductor laser, DBR semiconductor laser is sensitive to temperature. Therefore, a semiconductor laser control model including the influence of temperature is necessary, and this model should be able to fully reflect all the control characteristics of the semiconductor laser. Semiconductor laser control model is a nonlinear time-varying system, so it is not easy to establish a TFC model of DBR semiconductor laser that is applicable to atomic inertial measurement. The commonly used method in industrial control is to divide the operating range of the object into several independent working points, and express the dynamic characteristics of the object with transfer function near the working point [32]. The transfer function model is basically composed of the inertia part, the delay part, the integral part and the positive zero point part, as follows:

The stable process object:

$$G_{spo}(s) = \frac{k(1-as)}{(Ts+1)^n}e^{-\tau s}, \qquad (1)$$

77

and the non-self-balancing object:

$$G_{nsbo}(s) = \frac{k(1-as)}{s(Ts+1)^n}e^{-\tau s}, \qquad (2)$$

In the equation, n is the structural parameter, k, a, T and τ are the process parameters of the object. Their values depend

on the pecific system. In this paper, we first use the system identification toolbox in Matlab to fit the input and output data to obtain the initial parameters of the transfer function model of the laser. Then,the negative and positive absolute values of these initial parameters multiplying with a constant number a ($a \in [1, 10]$), are taken as the lower bound and upper bound of the value ranges of the corresponding parameters, respectively. For example, initial value of parameter k is k_o, the value range is $[-a * |k_0|, +a * |k_o|]$.

When the DBR semiconductor laser is modeled near the working point, we choose the above two modes as the alternative models. The control objective of the self-developed semiconductor laser system is to make the output wavelength and power of the laser stable by adjusting the input current and the input temperature of the semiconductor laser reasonably, so that the requirement to control the laser source in quantum instrument can be met. The most important content of the system is to obtain the relationship between laser frequency, power and its influencing factors, i.e. laser input current and temperature.

According to the above analysis, the semiconductor laser can be regarded as a dual input and dual output system. In the actual operation of semiconductor lasers, under the control of input current and temperature, the output wavelength and power of semiconductor laser are seriously coupled. At present, only one of them can be guaranteed to be stable in the closed-loop control of semiconductor lasers. When the wavelength is stable, the stability of semiconductor laser power is difficult to ensure. After the quantum instrument operates the light source stabilized on the saturated absorption lines of potassium atom, the power is attenuated to a certain stable value through a noise attenuator. The control system of this method is complex and a certain optical power will be lost. Therefore, a multi-input and multi-output system model is urgently needed to meet the control requirements.

The multi-input and multi-output model of DBR semiconductor laser is established as follows:

$$\begin{bmatrix} C \\ T \end{bmatrix} = G(s) \begin{bmatrix} P \\ W \end{bmatrix}, \tag{3}$$

In the equation 3, C is the laser input current, T is the laser temperature, P is the laser output power and W is the laser output wavelength. $G(s)$ is a 2×2 transfer function matrix which represent the coupling relationship between laser wavelength and power.

It can be seen from the equation (3) that the laser is a dual-input and dual-output system. According to its output characteristics, it is divided into two dual-input and single-output systems for modeling as shown in the figure below. Then each dual-input-single-output system can be considered as a superposition of two single-input-single-output (SISO) systems. For each SISO system, we can obtain the data reflecting the causal relationship between input and output according to identification test or experiment, and data processing is necessary to facilitate system identification. We can select a suitable model from the above model set, which
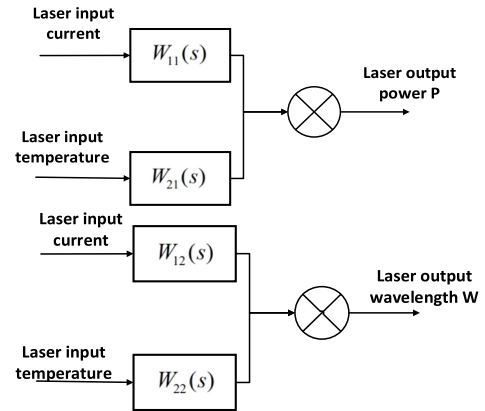

FIGURE 2. The near-working point TFC model of DBR semiconductor laser.

usually meets the principle of error minimization. In this paper, a quantum particle swarm optimization (QPSO) based modeling method is used to minimize the output of fitness function.

B. TFC MODEL RECOGNITION METHOD FOR LASER NEAR THE WORKING POINT

When the model set is determined as above and the input and output data are obtained, the TFC modeling of the laser near the working point is actually a problem of system identification. In the transfer function control model (equation 1 and equation 2) used in this paper, n is structural parameters and is identified by ergodic method. K, a, t and τ are process parameters identified by quantum particle swarm optimization algorithm. QPSO is an efficient quantum particle swarm optimization algorithm with the advantages of easy implementation, fast convergence and few parameters.

QPSO assumes that each particle has quantum behavior and describes the state of the particle by two wave functions. The square of the wave function represents the probability density of the particle appearing in space. The particle position is obtained by two steps. First, obtaining the probable distribution function of the particle position by solving the steady-state Schrodinger equation. Then, the position equation is obtained by Monte Carlo stochastic simulation. It can be seen that the QPSO algorithm cancels the orientation property of the particle, and the position of the particle has nothing to do with the previous movement, which increases the randomness of the particle position. Therefore, QPSO has better global search ability than PSO.

In order to make the model close to the actual system, the squared sum of differences between the model output and the actual output is chosen as the objective function in this paper as follow:

$$Y_{object}(x) = \sum_{i=1}^{N} (x_{\mod el}(i) - x_{actual}(i))^2, \tag{4}$$

In the equation, Y_{object} is the objective function, $x_{\mod el}$ is model output, x_{act} is actual output, N is the number of data points.

QPSO is different from PSO in updating the position of particles. The updating steps of QPSO are as follows:

Step 1: Calculate the best position of the average particle history *mbest*:

$$mbest(t) = \frac{1}{N} \sum_{i=1}^{N} pbest_i(t)$$

$$= (\frac{1}{N} \sum_{i=1}^{N} pbest_{i,1}(t), \frac{1}{N} \sum_{i=1}^{N} pbest_{i,2}(t), \cdots \frac{1}{N}$$

$$\times \sum_{i=1}^{N} pbest_{i,M}(t)), \qquad (5)$$

In the equation, N is the size of the particle swarm and M is the characteristic particle dimension.

Step 2: Update particle position:

$$X_{i,j}(t+1) = p_{i,j}(t) \pm \alpha * \left| mbest_j(t) - X_{i,j}(t) \right| * \ln(\frac{1}{u_{ji}(t)}), \qquad (6)$$

$$p_{i,j} = \varphi_j(t) * pbest_{i,j}(t) + \left[1 - \varphi_j(t)\right] * gbest_j(t), \qquad (7)$$

$$\alpha = 0.5 + \frac{(1 - 0.5)T_{max} - t}{T_{max}}, \qquad (8)$$

In the equation, $\varphi_i, u_{ij} \in U(0,1)$, *mbest* is historically optimal location of average particles. After t times iteration, $pbest_{i,j}(t)$ is j-dimensional coordinate value at the current optimum position of particle i, $gbest_i(t)$ is j-dimensional coordinate value of global optimum position. α is a contraction-expansion coefficient, usually fixed or decreasing in a certain range.

III. EXPERIMENT

The identification process of TFC model of DBR laser near the working point is shown in the following FIGURE 3. Firstly, the laser is operated at the working point for a period of time (2 hours) to achieve a stable state. Then, excitation signals are added to the laser, and the voltage signals corresponding to the input and output signals of the laser are collected synchronously. After pretreatment, we use the processed data to model the transfer function of DBR laser, optimize the parameters of the model through QPSO algorithm, and finally obtain the TFC model to meet the demand.

A. DATA ACQUISITION AND PREPROCESSING

Since the light sources used in quantum instruments usually work at the resonance frequencies of the controlled atoms. In this paper, the input of the laser for saturated absorption frequency stabilization is selected as the input of the working point. It should be noted that the input excitation signal at the working point should induce obvious output response of the laser as far as possible, but it should not be too large which will cause mode adjustment of the laser. The working point selected in this paper corresponds to a temperature of 25.7°C and a current of 79 mA. The excitation input
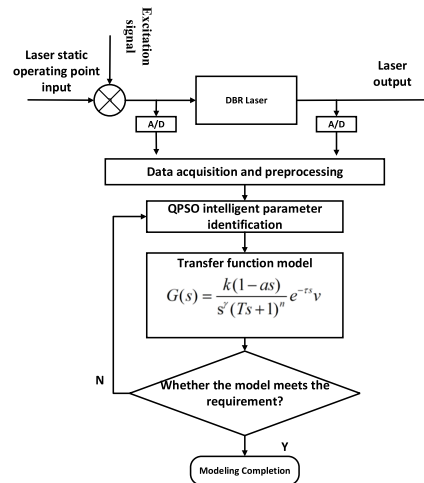

FIGURE 3. Schematic diagram of identification process for the TFC model at near-working point.
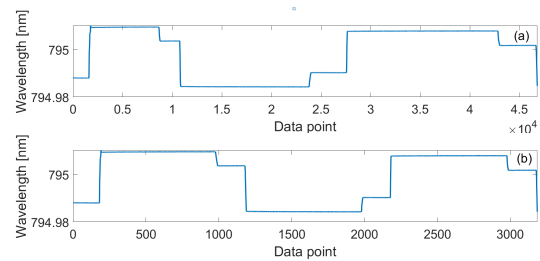

FIGURE 4. Contrast diagram of the wavelength data of laser output before and after the secondary sampling.

is about 5 mA and the excitation temperature is 0.35°C. In this paper, the artificial periodic excitation signal is used to add the excitation signal in a period of about 5 minutes. Because of the homemade laser controller, the time of current regulation is much shorter than that of temperature control. In order to reduce the interaction between current excitation and temperature excitation as much as possible, the sequence of excitation signals is as follows: We first add current excitation, and then add temperature excitation after a minute. Four minutes later, the excitation current is removed, and another one minute later, the temperature excitation is removed. This completes a set of data acquisition. In order to ensure the accuracy of the model, we collected a number of groups of data. The wavelength meter used in the experiment is WS7, the sampling period changes with time when collecting data (show as FIGURE 4a), so it needs to be processed and synchronized with other data. The maximum interval between the recorded data of the wavelength meter is about 100 ms. The synchronization of modeling data determines the accuracy and reliability of the model, we developed a new data processing method that can deal with time varying sampling periods by re-sampling. In order to fix the sampling frequency and reproduce the original data, we use a period of 330 ms to re-sample the wavelength data. The specific process is as follows:

1. Determine the time axis: Determine the total sampling time of the wavelength data, and interpolate it with a period of 330ms to obtain a new time axis.

2. Obtain the data corresponding to the corresponding time points of the new time axis: Search the data points in the time data corresponding to the new time axis, and select the data closest to the time as the data corresponding to the corresponding time points of the new time axis. The processed modeling data is shown in FIGURE 4b.

The zero of the unprocessed identification data is arbitrary or zero-crossing. In order to facilitate pattern recognition, the data need to be processed as follows:

$$
\begin{cases}
u^*(k) = u(k) - \dfrac{1}{N}\sum_{i=1}^{N} u(i) \\
y^*(k) = y(k) - \dfrac{1}{N}\sum_{i=1}^{N} y(i),
\end{cases}
\tag{9}
$$

N is the number of data points in the equation, $u(k)$ is input data, $y(k)$ is output data.
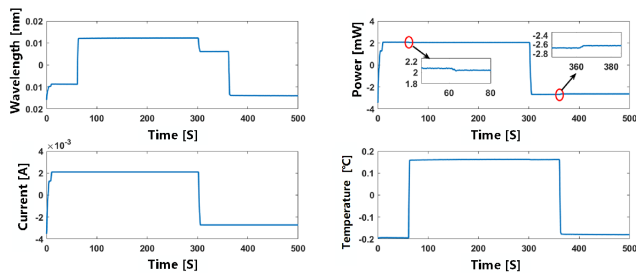

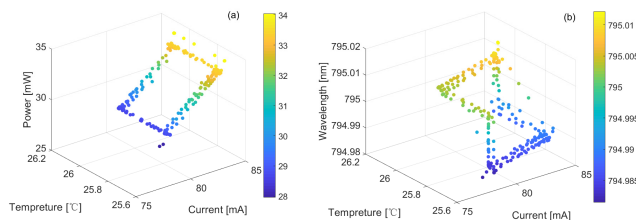**FIGURE 5. Data processed for model parameter identification.**

FIGURE 6. The power and wavelength responses of the laser to the input: (a) Power response (b) Wavelength response.

FIGURE 5 shows that the laser output has a significant linear correlation with the current and the temperature of laser input at near-working point. This provides an experimental basis for the decomposition of the multi-input multi-output DBR semiconductor laser TFC model into two main modules: the laser power control module and the laser wavelength control module. FIGURE 6(a) illustrates that the power response is approximately linearly correlated with the current and the temperature of laser input, and there is no cross or nonlinear coupling between the power response to the input current and the power response to the input temperature. FIGURE 6(b) shows that the wavelength response is also approximately linearly correlated with the current and the

TABLE 1. The laser near-working point TFC model.

Variable	Laser output power	Laser output wavelength
Laser input current	$W_{11}(s)=\dfrac{977.4801}{0.0000590s+1}*e^{-0.1001}$	$W_{12}=\dfrac{9.218s-0.000238}{s^2+7.309s+0.000101}e^{-0.01s}$
Laser temperature	$W_{21}=\dfrac{-0.1168}{2.0420s+1}*e^{-1.3194s}$	$W_{22}(s)=\dfrac{0.00862s+0.0095}{s^2+0.622s+0.1615}e^{-0.05s}$

temperature of laser input, but there certainly exists a cross coupling between the wavelength responses to the current and the temperature of laser input.

B. INTELLIGENT IDENTIFICATION OF THE TFC MODEL AND MODEL TEST

According to the above analysis, n is a structural parameter in the alternative model. In this paper, ergodic method is used. Because in practical application, most of the systems can be represented by first-order or second-order systems. So $n \in [1-3]$. k, a, t, τ which belong to process parameters, are identified by quantum particle swarm optimization algorithm. At first, we select a set of data with large initial parameter intervals for system identification. Generally, the result of QPSO identification is unsatisfactory. If the result of QPSO identification does not meet the requirement, it is necessary to modify the interval of identification parameters which have reached the upper or lower limit several times until a set of acceptable parameters is obtained. The TFC model obtained by simulation optimization is as Table1, and the identification results are as FIGURE 7 and FIGURE 8.
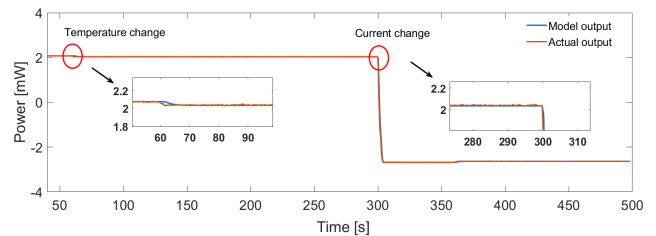

FIGURE 7. The output of the identified power model and the actual power output at near-working point.
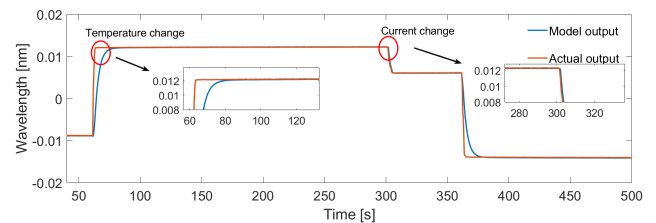

FIGURE 8. The output of the identified wavelength model and the actual wavelength output at near-working point.

As for the laser power control module, FIGURE 6 illustrates the output of the identified power model and the actual power output at near-working point. When the transition period caused by abrupt temperature change ends, where the

difference between the output of the identified power model and the actual power output is observable, the laser system enters the steady state, where the two outputs coincide with each other well. Besides, the output of the identified power TFC model coincides well with the actual power output at both the steady state period and the transition period caused by abrupt current change. For both the temperature and current responses, the error standard deviation (ESD) of the TFC model output corresponding to the laser power control module is 0.061.

For the laser wavelength control module, the output of the identified wavelength model shows similar pattern when temperature changes abruptly as show in FIGURE 7. When the transition period caused by abrupt temperature change ends and the laser system enters the steady state, the output of the identified wavelength TFC model coincides well with the actual wavelength output. Besides, the output of the identified wavelength TFC model coincides well with the actual wavelength output at both the steady state period and the transition period caused by abrupt current change. For both the temperature and current responses, the error standard deviation (ESD) of the wavelength TFC model output corresponding to the laser power control module is 0.001. The model to verify whether the identified transfer function can correctly characterize the input and output characteristics of DBR laser is validated as below.

IV. MODEL VALIDATION

Five sets of test data are used to verify the feasibility and effectiveness of the model. FIGURE 9 shows the output error result of the laser power control module of the DBR laser near the working point. It can be seen in the figure that the ESD of the identified power model of the fifth group of test data is at least 0.0607. The average ESD of the identified power model output of the five groups of data is 0.0659; And the fourth group of test data obtained the minimum ESD of the identified power model steady-state output (0.0027), which means the steady-state output error is 42.3 times smaller. The average steady-state output ESD of the laser power control module is 0.0034. FIGURE 10 shows error result of the laser wavelength control module of the DBR laser near the working point. The second set of test data has the lowest the ESD of the identified wavelength model output (6.3728×10^{-4}) and the third set of data has the lowest ESD of the identified wavelength model steady-state output (1.1552×10^{-5}). The mean of the above two ESD of the identified wavelength model is 0.0011 and 1.2807×10^{-5} respectively, which are 87 times different from each other. It can be seen from the above analysis results that the ESD of the identified model output is not as good as the ESD of the identified model steady-state output .This may be due to the fact that the actual laser input temperature control system is not ideal and the temperature modulation cannot be completed instantaneously. However, in practical applica-tion, the steady-state response of the model is mainly concerned.
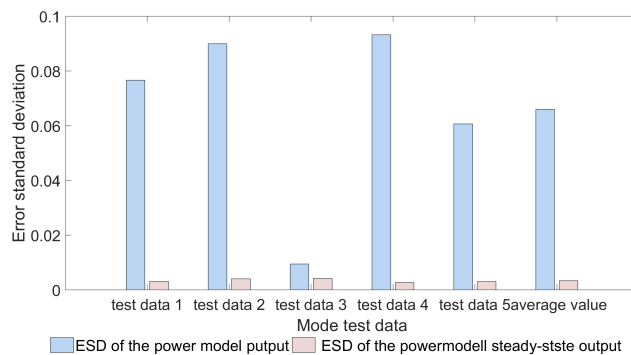

FIGURE 9. Error standard deviation results of power TFC model at near-working point.
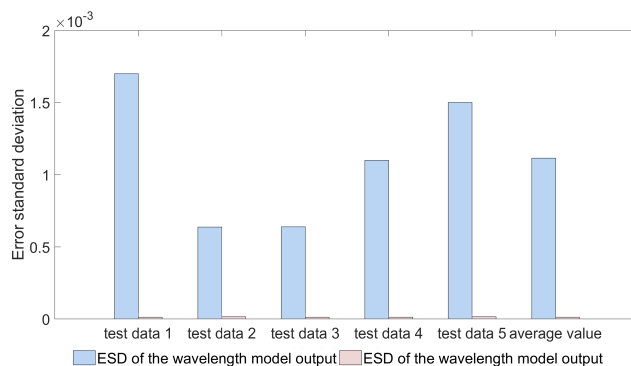

FIGURE 10. Error standard deviation results of wavelength TFC model at near-working point.

In conclusion, the proposed model can well simulate the steady state response of the laser near the working point, while the transient response of the laser near the working point is slightly worse. By comparing the output of the model with the actual output of the laser, it can be seen that the identification result is ideal, the output curve of the model fits well with the output curve of the actual process. The two-input-two-output TFC model obtained by multi-variable system identification can better characterize the actual dynamic characteristics of the DBR laser near the working point. Briefly, the identified model is effective and feasible.

V. CONCLUSION

In this paper, we analyzed the input-output characteristics of a self-developed DBR laser at near-working point, where the laser system can be equivalent to a TFC model including two main modules: the laser power control module and the laser wavelength control module. These two modules fully reflect all the control characteristics of the laser system at near-working point. To satisfy the prerequisite of the model identification for transfer function control, we developed a new data processing method that can deal with time vary-ing sampling periods, which is applied in the process of identification data preprocessing. Then, the model param-eters are identified by using the QPSO algorithm, and the

near-working point TFC model of the DBR laser with home-made controller is obtained. Experiments illustrated that this model can fully reflect the control characteristics of the DBR laser at near-working point.

The contributions of our modeling method are that: it can provide the mathematical basis and the simulation model to optimize the subsequently developed laser controllers; it can be applied for the wavelength-power decoupling control of the self-developed DBR laser systems; it is simple, effective and easy apply to the semiconductor laser systems; it can be used for online modeling and optimization of the near-working point transfer function control of DBR laser systems, such that the laser output's power and wavelength can be more stable. By extension, this modeling method can also provide a reference for the TFC modeling of other types of lasers at near-working point.

REFERENCES

[1] J. Fang and J. Qin, "Advances in atomic gyroscopes: A view from inertial navigation applications," *Sensors*, vol. 12, no. 5, pp. 6331–6346, May 2012.

[2] S. Karlen, G. Buchs, T. Overstolz, N. Torcheboeuf, E. Onillon, J. Haesler, and D. Boiko, "MEMS atomic vapor cells for gyroscope applications," Presented at the Joint Conf. Eur. Freq. Time Forum IEEE Int. Freq. Control Symp. (EFTF/IFCS), Jul. 2017. [Online]. Available: https://ieeexplore. ieee.xilesou.top/abstract/document/8088879/metrics#metrics

[3] I. K. Kominis, T. W. Kornack, J. C. Allred, and M. V. Romalis, "A subfemtotesla multichannel atomic magnetometer," *Nature*, vol. 422, no. 6932, pp. 596–599, Apr. 2003.

[4] C. Deans, L. D. Griffin, L. Marmugi, and F. Renzoni, "Machine learning based localization and classification with atomic magnetometers," *Phys. Rev. Lett.*, vol. 120, no. 3, Jan. 2018, Art. no. 033204.

[5] A. D. Ludlow, M. M. Boyd, J. Ye, E. Peik, and P. O. Schmidt, "Optical atomic clocks," *Rev. Mod. Phys.*, vol. 87, no. 2, pp. 637–701, Jun. 2015.

[6] T. E. Mehlstäubler, G. Grosche, C. Lisdat, P. O. Schmidt, and H. Denker, "Atomic clocks for geodesy," *Rep. Prog. Phys.*, vol. 81, no. 6, Jun. 2018, Art. no. 064401.

[7] J. Le Gouët, T. Mehlstäubler, J. Kim, S. Merlet, A. Clairon, A. Landragin, and F. Pereira Dos Santos, "Limits to the sensitivity of a low noise compact atomic gravimeter," *Appl. Phys. B, Lasers Opt.*, vol. 92, no. 2, pp. 133–144, Aug. 2008.

[8] Q. Luo, H. Zhang, K. Zhang, X.-C. Duan, Z.-K. Hu, L.-L. Chen, and M.-K. Zhou, "A compact laser system for a portable atom interferometry gravimeter," *Rev. Sci. Instrum.*, vol. 90, no. 4, Apr. 2019, Art. no. 043104.

[9] C. Elouard, D. A. Herrera-Martí, M. Clusel, and A. Auffèves, "The role of quantum measurement in stochastic thermodynamics," *npj Quantum Inf.*, vol. 3, no. 9, pp. 1–10, Mar. 2017.

[10] A. Acín, I. Bloch, H. Buhrman, T. Calarco, C. Eichler, J. Eisert, D. Esteve, N. Gisin, S. J. Glaser, F. Jelezko, S. Kuhr, M. Lewenstein, M. F. Riedel, P. O. Schmidt, R. Thew, A. Wallraff, I. Walmsley, and F. K. Wilhelm, "The quantum technologies roadmap: A European community view," *New J. Phys.*, vol. 20, no. 8, Aug. 2018, Art. no. 080201.

[11] C. Elouard and A. N. Jordan, "Efficient quantum measurement engines," *Phys. Rev. Lett.*, vol. 120, no. 26, Jun. 2018, Art. no. 260601.

[12] M. Morishita, T. Ohmi, and J. Nishizawa, "Impedance characteristics of double-heterostructure laser diodes," *Solid-State Electron.*, vol. 22, no. 11, pp. 951–962, Nov. 1979.

[13] R. S. Tucker, "Circuit model of double-heterojunction laser below threshold," *IEE Proc. I-Solid-State Electron. Devices*, vol. 128, no. 3, pp. 101–106, Jun. 1981.

[14] J. Katz, S. Margalit, C. Harder, D. Wilt, and A. Yariv, "The intrinsic electrical equivalent circuit of a laser diode," *IEEE J. Quantum Electron.*, vol. QE-17, no. 1, pp. 4–7, Jan. 1981.

[15] R. S. Tucker, "Large-signal circuit model for simulation of injection-laser modulation dynamics," *IEE Proc. I-Solid-State Electron Devices*, vol. 128, no. 5, pp. 180–184, Oct. 1981.

[16] R. Tucker and D. Pope, "Circuit modeling of the effect of diffusion on damping in a narrow-stripe semiconductor laser," *IEEE J. Quantum Electron.*, vol. QE-19, no. 7, pp. 1179–1183, Jul. 1983.

[17] R. S. Tucker and D. Pope, "Microwave circuit models of semiconductor injection lasers," *IEEE Trans. Microw. Theory Techn.*, vol. MTT-31, no. 3, pp. 289–294, Mar. 1983.

[18] T. P. Lee, "Effect of junction capacitance on the rise time of LED's and on the turn-on delay of injection lasers," *Bell Syst. Tech. J.*, vol. 54, no. 1, pp. 53–68, Jan. 1975.

[19] J. Gao, "An analytical method to determine small-signal model parameters for vertical-cavity surface emitting lasers," *J. Lightw. Technol.*, vol. 28, no. 9, pp. 1332–1337, May 1, 2010.

[20] M. Bruensteiner and G. Papen, "Extraction of VCSEL rate-equation parameters for low-bias system simulation," *IEEE J. Sel. Topics Quantum Electron.*, vol. 5, no. 3, pp. 487–494, May/Jun. 1999.

[21] B. Fetics, E. Nevo, C.-H. Chen, and D. Kass, "Parametric model derivation of transfer function for noninvasive estimation of aortic pressure by radial tonometry," *IEEE Trans. Biomed. Eng.*, vol. 46, no. 6, pp. 698–706, Jun. 1999.

[22] F. J. Nogales and A. J. Conejo, "Electricity price forecasting through transfer function models," *J. Oper. Res. Soc.*, vol. 57, no. 4, pp. 350–356, Apr. 2006.

[23] W. A. Jury, G. Sposito, and R. E. White, "A transfer function model of solute transport through soil: 1. Fundamental concepts," *Water Resour. Res.*, vol. 22, no. 2, pp. 243–247, Feb. 1986.

[24] J. P. Guigay, M. Langer, R. Boistel, and P. Cloetens, "Mixed transfer function and transport of intensity approach for phase retrieval in the Fresnel region," *Opt. Lett.*, vol. 32, no. 12, p. 1617, Jun. 2007.

[25] J. Sun, W. Fang, X. Wu, V. Palade, and W. Xu, "Quantum-behaved particle swarm optimization: Analysis of individual particle behavior and parameter selection," *Evol. Comput.*, vol. 20, no. 3, pp. 349–393, Sep. 2012.

[26] J. Sun, W. B. Xu, W. Fang, "Quantum-behaved particle swarm optimization with a hybrid probability distribution," presented at the Pricai Trends Artif. Intell., Aug. 2016. [Online]. Available: https://link.springer. xilesou.top/chapter/10.1007/978-3-540-36668-3_78.

[27] L. D. S. Coelho, "Gaussian quantum-behaved particle swarm optimization approaches for constrained engineering design problems," *Expert Syst. Appl.*, vol. 37, no. 2, pp. 1676–1683, Mar. 2010.

[28] C. Sun and S. Lu, "Short-term combined economic emission hydrothermal scheduling using improved quantum-behaved particle swarm optimization," *Expert Syst. Appl.*, vol. 37, no. 6, pp. 4232–4241, Jun. 2010.

[29] S. Ch, N. Anand, B. Panigrahi, and S. Mathur, "Streamflow forecasting by SVM with quantum behaved particle swarm optimization," *Neurocomputing*, vol. 101, pp. 18–23, Feb. 2013.

[30] E. C. Honea, S. J. A. Kidmore, B. L. Freitas, E. J. Utterback, and M. A. Emanuel, "Modeling the effect of heatsink performance on high-peak-power laser-diode-bar pump sources for solid state lasers," *Optoelectron. High-Power Lasers Appl.*, vol. 3285, pp. 178–189, May 1998.

[31] L. Bjerkan, A. Royset, L. Hafskjaer, and D. Myhre, "Measurement of laser parameters for simulation of high-speed fiberoptic systems," *J. Lightw. Technol*, vol. 14, no. 5, pp. 839–850, May 1996.

[32] L.-M. Liu and D. M. Hanssens, "Identification of multiple-input transfer function models," *Commun. Statist.-Theory Methods*, vol. 11, no. 3, pp. 297–314, Jan. 1982.

XIUFEI LI is currently pursuing the Ph.D. degree with the School of Instrumentation Science and Opto-Electronics Engineering, Beihang University.

His current research interests are quantum precision measurement and sensing technology, and control technology of high-stability laser source.

ZHUO WANG (Member, IEEE) was born in Handan, Hebei, China, in 1983. He received the B.E. degree in automation from Beihang University, Beijing, China, in 2006, and the Ph.D. degree in electrical and computer engineering from the University of Illinois at Chicago, Chicago, IL, USA, in 2013.

He was a Postdoctoral Fellow with the Department of Electrical and Computer Engineering, University of Alberta, from 2013 to 2014. He worked as a Research Assistant Professor with the Fok Ying Tung Graduate School, Hong Kong University of Science and Technology, from 2014 to 2015. He was selected for the 12th Recruitment Program for Young Professionals by the Organization Department of the CPC Central Committee and the 100 Talents Program by Beihang University, in 2015. He is currently a Professor and a Ph.D. Instructor with the Beijing Academy of Quantum Information Sciences, Beijing, with the Research Institute for Frontier Science, Beihang University, and with the Key Laboratory of the Ministry of Industry, Beihang University.

LU YU received the B.S. degree in detection, guidance, and control from Beihang University, Beijing, China, in 2018, where she is currently pursuing the M.S. degree in precision instrument.

She is also a Graduate working with the Science and Technology on Initial Laboratory, Beihang University. Her research interest includes the non-contact temperature measurement based on saturated absorption spectroscopy and temperature control of semiconductor laser.

XIAOLIN NING was born in Jinan, China, in 1979. She received the B.E. degree in computer science from Shandong Normal University, Shandong, in 2001, and the Ph.D. degree in mechanical engineering from Beihang University, Beijing, in 2008.

She has been a Professor with Beihang University, since 2011. She is currently a Ph.D. Instructor with the Beijing Academy of Quantum Information Sciences, and with the Research Institute for Frontier Science, Beihang University. Her research interests include guidance, navigation, and control system of spacecrafts.

WEI QUAN received the Ph.D. degree of precision instrument and mechanics from Beihang University, China, in 2008.

He is currently working with the Beijing Academy of Quantum Information Sciences, Beijing, with the Research Institute for Frontier Science, Beihang University, Beijing, and with the Key Laboratory of the Ministry of Industry, Beihang University. His current research interests are atomic spin inertial measurement, atomic magnetic field measurement, and information fusion navigation.
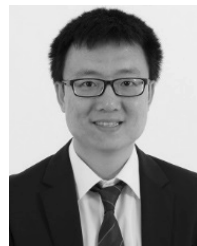
YUEYANG ZHAI received the M.S. and Ph.D. degree from the School of Electronics Engineering and Computer Science, Peking University, China, in 2018 and 2013, respectively.

He is currently an Associate Professor with the Beijing Academy of Quantum Information Sciences, Beijing, and with the Research Institute for Frontier Science, Beihang University, Beijing. His research fields including atomic molecular optics, quantum sensors, cold atom, and quantum simulation. His current research interest is atomic precision measurement.

• • •